Proceedings of the 9th U.S. National and 10th Canadian Conference on Earthquake Engineering
Compte Rendu de la 9ième Conférence Nationale Américaine et
10ième Conférence Canadienne de Génie Parasismique
July 25-29, 2010, Toronto, Ontario, Canada • Paper No 1008

DYNAMIC TESTS OF 0.76 & 0.91 MM STEEL DECK DIAPHRAGMS FOR SINGLE-STOREY BUILDINGS

J. Franquet[1], R. Massarelli[1], K. Shrestha[1], R. Tremblay[2] and C.A. Rogers[3]

ABSTRACT

An experimental program was carried out to assess the dynamic characteristics of roof deck diaphragm assemblies. Eight 7.31 m x 21.02 m specimens were subjected to broadband, single frequency and seismic excitations in the elastic range to determine the fundamental period, resonance and elastic seismic response, respectively. In addition, each specimen was subjected to an inelastic loading protocol to evaluate its inelastic performance. Deck thicknesses of 0.76 mm and 0.91 mm were used for the purpose of this investigation. Connection configurations comprised powder-actuated nails and screws as well as arc spot welds and button-punches. The tests showed a decrease in shear stiffness with increasing excitation amplitude and an overestimation of the stiffness for dynamic loading conditions in comparison to current diaphragm design methods. The tests also showed that satisfactory ductile behaviour can be achieved with 0.76 mm nailed and screwed diaphragms but not necessarily with 0.91 mm nailed and screwed diaphragms or welded and button-punched specimens. Repair strategies for diaphragms that have previously undergone inelastic deformations were also devised in an attempt to restore the original in-plane shear stiffness and strength.

Introduction

Engineers often rely on the steel roof deck to act as a diaphragm in the seismic force resisting system (SFRS) of a single-storey building. The diaphragm is designed to transfer the inertia loads, through shearing action, to the bracing bents of the structure. This in-plane load transferring capability is achieved by connecting the steel deck panels together as well as to the underlying frame. The chord and collector elements also greatly contribute to the load transferring system. Model building codes base the calculation of equivalent static seismic forces on the characteristics (stiffness, ductility and overstrength) of the vertical lateral system without consideration of this roof system. It has been demonstrated by analytical means that accounting for the in-plane flexibility of the roof diaphragm allows for a longer period of vibration of the building, which results in lower seismic loads for design (Tremblay et al. 2002; Tremblay & Rogers 2005; Rogers & Tremblay 2010). However, recent ambient vibration studies have shown that the period of vibration may be shorter than that predicted by analytical means (Tremblay et al. 2008b; Lamarche et al. 2009).

A limited number of dynamic diaphragm tests carried out in 2007 illustrated that the in-

[1]Graduate Research Assistant, Dept. of Civil Eng. and Applied Mechanics, McGill University, Montreal, Canada
[2]Professor, Dept. of Civil, Geological and Mining Eng., École Polytechnique de Montreal, Montreal, Canada
[3]Associate Professor, Dept. of Civil Eng. and Applied Mechanics, McGill University, Montreal, Canada

plane shear stiffness of the roof assembly decreases as the amplitude of vibrations increases (Tremblay et al. 2008a). This preliminary information indicates that the use of ambient vibration tests to evaluate the period of low rise buildings may not provide representative stiffness characteristics for use in the seismic design of a structure that is expected to undergo strong ground motion shaking. Furthermore, the use of capacity based design concepts, as documented in the National Building Code of Canada (NRCC 2005), require the diaphragm to be designed for the probable capacity of the brace members. This has resulted in the need for much thicker deck and significantly more connectors, which has elevated the cost of construction (Tremblay & Rogers 2005) and in some cases has restricted the use of roof diaphragms because of inadequate shear resistance. The stiffness and inelastic deformation characteristics of roof deck diaphragms when subjected to representative ground motions needed to be identified such that design recommendations could be made with respect to determining the period of vibration of single-storey steel buildings as well as the possibility of defining the roof system as the inelastic fuse. This necessitated the completion of large-scale diaphragm tests in which both the ductility and change in stiffness with respect to excitation could be measured.

Large-Scale Diaphragm Test Program

Test Setup

A test program was carried out on eight 7.31 m x 21.02 m metal roof deck diaphragm specimens (Figure 1) subjected to dynamically applied in-plane loading (Franquet 2010). Standard 0.76 mm and 0.91 mm thick 38 mm deep roof deck panels supported on roof beam and joist elements formed the diaphragm specimens. Nail frame connections and screw side-lap connections were used for all of the specimens except one, which was fastened using puddle welds and button punch sidelaps. The intent was to replicate the common diaphragm configurations found in construction. The tests were conducted at different amplitudes of loading to characterize the dynamic properties from elastic to inelastic response.

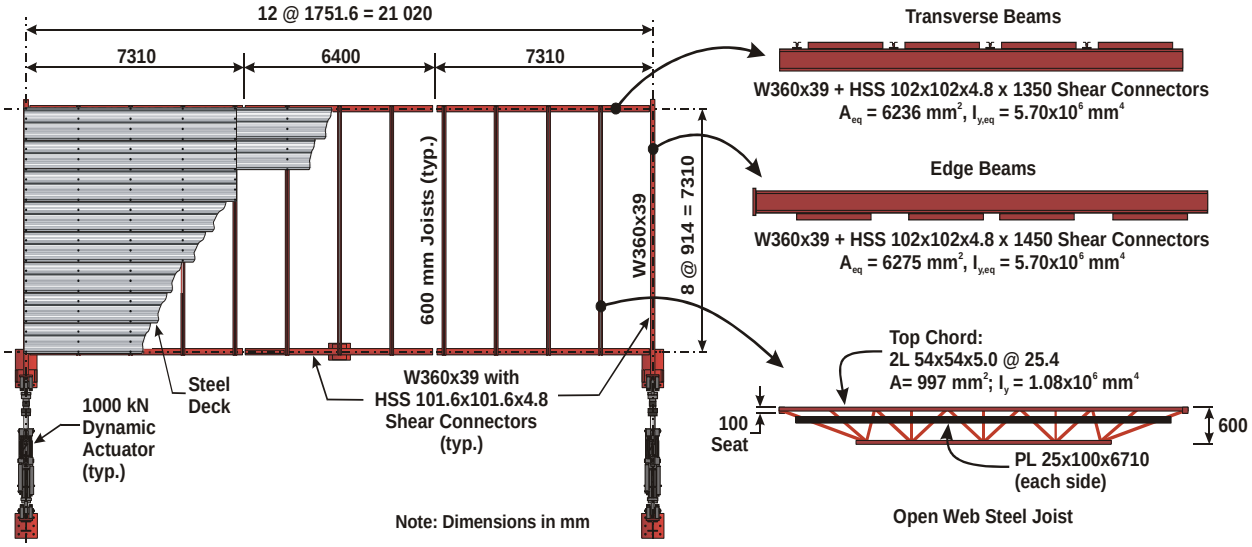

Figure 1. Diaphragm test frame layout

The eave and collector beams were composed of W360x39 sections. Eleven typical open-web steel joists completed the frame and were placed 1.75 m o/c. The joists were designed to

carry a maximum unfactored dead load of 2.12 kN/m and live load of 3.8 kN/m. A design depth of 600 mm was also used to mimic typical joists in long span building applications. These also had a 100 mm seat for direct support on the W-beams. Shear connectors composed of HSS 102 x 102 x 4.8 were welded on the eave beams to allow for frame connections at those locations. Two 1000 kN high performance dynamic MTS actuators were used on either side of the frame to induce in-phase and in-plane loading on the diaphragm specimens. The frame was supported on rockers placed symmetrically along the width. Steel masses were distributed evenly on the deck to provide an additional dead load of 0.18 kPa. As well, four 25 x 100 x 6710 mm steel plates were welded to each side of the joists to add mass, and consequently inertia forces, to ensure that inelastic behaviour would occur. These plates totalled a supplementary 117.3 kN in the overall frame weight of 202.3 kN.

Specimens

The specimens consisted of 0.76 mm thick Z275 (G90) galvanized steel corrugated decking complying to ASTM A653 with 38 mm wide flutes spaced 152 mm apart. Two profiles, namely CANAM P-3606 for all nailed and screwed diaphragms and P-3615 for the welded and button-punched diaphragm were used (Figure 2a, Table 1).

a) b)

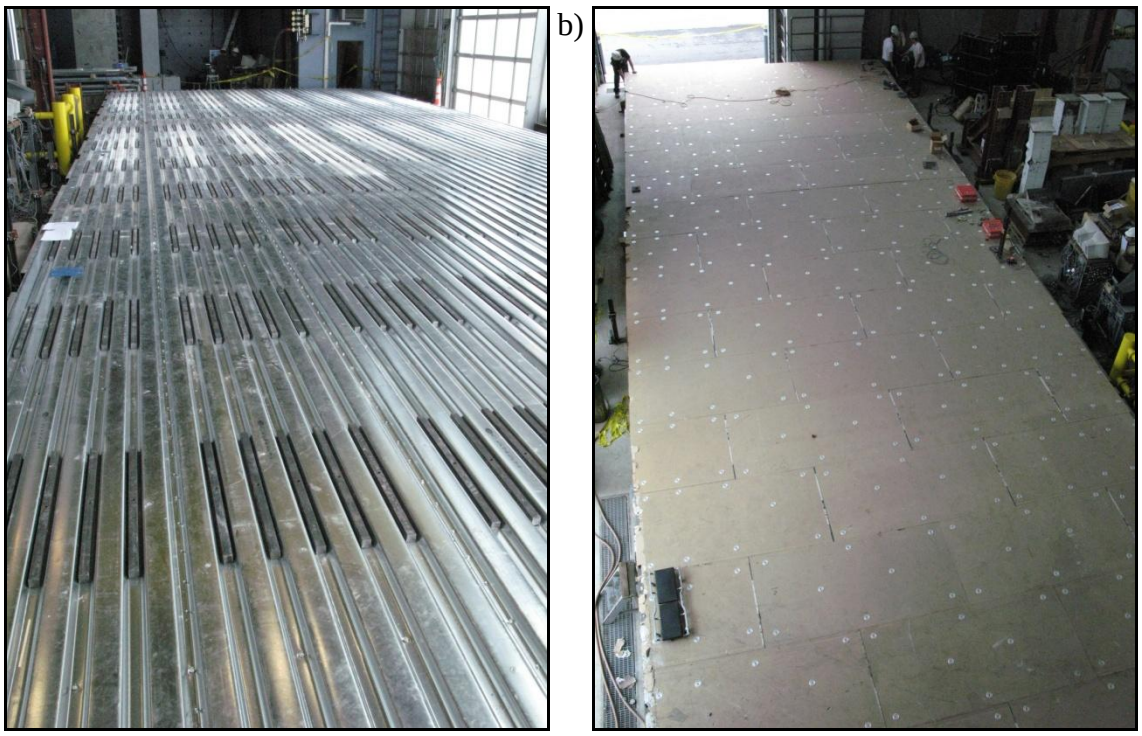

Figure 2. Typical diaphragm test specimens prior to testing.

The nominal material properties of the steel deck sheets were as follows; F_y = 230 MPa and F_u = 310 MPa. Coupon tests were performed to determine the actual material strengths (Franquet 2010). Nail fasteners were used to connect the deck panels to the underlying frame while Hilti S-MD 12-14x1M self-tapping screws were used to connect the sheets together. Two types of nails were used; Hilti type X-EDNK22 THQ12 for all joists and shear connectors while

X-EDN 19 THQ 12M nails were used for the frame connectors at the edge beam locations.

The welded diaphragm comprised 16 mm arc-spot welds (E6011 electrode) and button punches. An average measured weld diameter of 17 mm and an average welding time per connection of 7.3 sec were recorded. A seam locking tool was used to install the button punched connections at sidelap locations.

To investigate the influence of non-structural materials on the stiffness of the diaphragm system, gypsum was installed on the first specimen (DIA3) (Table 1, Figure 2b). The other components typically found in a roofing membrane were ignored as previous studies had shown that they did not influence the stiffness of the steel roof deck diaphragm (Tremblay et al. 2004; Mastrogiuseppe et al. 2008). The non-structural gypsum used in the testing program was standard Type X 5/8 inch gypsum board which was connected to the decking using screws with plate washers (Franquet 2010).

Table 1. Test program matrix

Test No.[1]	Deck Profile	Sheet Thickness (mm)	Frame Fasteners[2]	Fastener Pattern	End Overlap	Sidelap Fasteners	Sidelap Spacing (mm)
DIA3	38x914	0.76	ENDK22 Nails	36/4	36/7	#12 Screws	152
R			ENDK22 Nails	36/7	36/7	#12 Screws	152
DIA4	38x914	0.76	ENDK22 Nails	36/7	36/7	#12 Screws	152
R			ENDK22 Nails	36/9	36/9	#12 Screws	152
DIA5	38x914	0.76	ENDK22 Nails	36/9	36/9	#12 Screws	152
R			ENDK22 Nails	36/9	36/9	#12 Screws	102
DIA6	38x914	0.76	ENDK22 Nails	36/11	36/11	#12 Screws	152
R			ENDK22 Nails	36/11	36/11	#12 Screws	102
DIA7	38x914	0.91	ENDK22 Nails	36/7	36/7	#12 Screws	152
R			ENDK22 Nails	36/7	36/7	Rivets	152
DIA8	38x914	0.91	ENDK22 Nails	36/9	36/9	#12 Screws	152
R			ENDK22 Nails	36/9	36/9	#12 Screws	102
DIA9	38x914	0.91	ENDK22 Nails	36/11	36/11	#12 Screws	152
R			ENDK22 Nails	36/11	36/11	#12 Screws	102
DIA10	38x914	0.76	16 mm welds	36/4	36/4	Button punch	305
R	38x914	0.76	ENDK22 Nails	36/4	36/4	#12 Screws	305

[1] R specimens refer to the previous specimen being repaired in an attempt to restore its strength and stiffness.
[2] ENDK22 nails used at transverse beams and joists; X-EDN 19 nails used at edge beam locations

The configurations of repaired diaphragm specimens are also listed in Table 1. Typically, damaged sidelap screw fasteners were replaced with additional screws and nails were installed adjacent to deck-to-frame connections that had undergone inelastic deformations. The sidelaps of Specimen DIA7 were repaired / replaced using blind rivets of type G-bulb GSMD85SGB. The intent was to evaluate the viability of these connectors in this type of building application. The weld / button punch specimen DIA10 was repaired using nails and sidelap screws.

Loading Protocols

Each of the diaphragm specimens was subjected to five types of signals: broadband excitations (white noise) (BB), single-frequency excitations (BF) seismic excitations (SS1 and SS3), and a protocol to bring the diaphragm into inelastic behaviour (SS2 or SS3). The broadband excitation consisted of a random signal with the same energy content over a range of frequencies. The bandwidth used in the context of testing ranged from 0 to 25 Hz. This signal was amplified until either the force reached 20% of the nominal resistance, as predicted using the SDI Design Manual (Luttrell, 2004) or a root-mean-square (RMS) acceleration response of 0.2 g was reached at the centre of the diaphragm span. The natural frequency could then be determined at different excitation amplitudes to observe the change in dynamic properties of the deck.

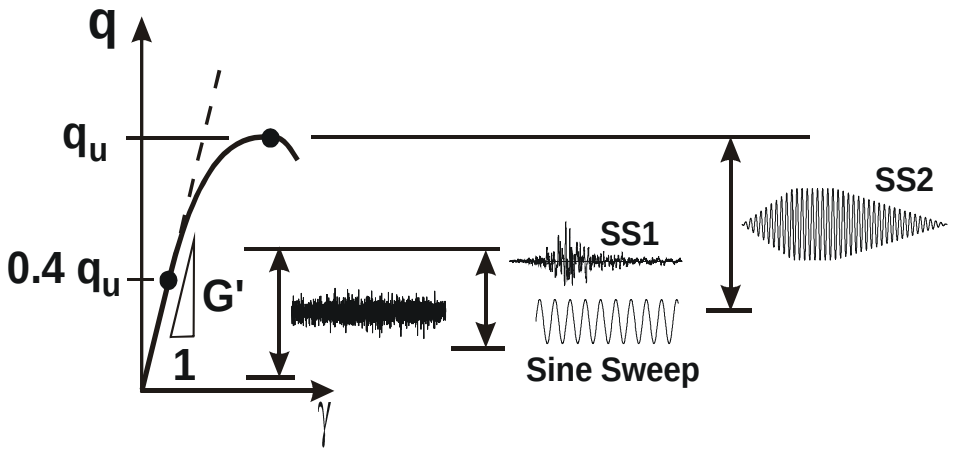

Figure 3. Representative dynamic loading protocols.

Single-Frequency (sine sweep) excitation was then applied over a range of frequencies surrounding the first mode. The acceleration was kept constant over the frequency range so that the input force would remain equal. A total of eight acceleration levels were used at each frequency. Resonance curves, which again show the change in dynamic properties of the diaphragm specimen, could then be obtained and damping could be derived from those same results. A limit of 20% of the nominal shear resistance was applied for these tests. The single-frequency tests were only possible for specimens with first mode natural periods of less than 7 Hz because the actuator performance was inadequate for higher frequency protocols.

Two seismic signals were used as loading protocols. Seismic signal SS1 is an acceleration record from the 1989 Loma Prieta earthquake (Stanford Univ. 360°) with a peak value of 0.29 g. A time scale factor of 1/3 was used to reflect the difference between the fundamental period of the test specimens and that of actual low-rise buildings. Seismic signal SS3 is an acceleration record from the Northridge Earthquake (Big Tujunga, 352°) with a peak value of 0.245 g. A time factor of 1/2.5 was applied to this ground motion record.

As a final test each of the specimens was subjected to a protocol devised to bring the diaphragm into inelastic behaviour. The signal (SS2) consisted of sine waves linearly increasing in amplitude until a four peak maximum amplitude was reached. The amplitude and frequency of this protocol were determined numerically with a truss model developed by Shrestha et al. (2009) which had been calibrated using the natural frequency obtained experimentally from the previous white noise tests. The ground motion acceleration record SS3 was originally used for

DIA3 and DIA3R in place of SS2 but the lack of complete inelastic shear force vs. deformation hysteresis curves made it inadequate for the calibration of a numerical model. The SS2 loading protocol was used for all other specimens.

Post-Processing

The natural frequencies at different root-mean-squared (RMS) acceleration values were determined from the white noise, or broadband excitation, test results using the Frequency Domain Decomposition (FDD) algorithm described by Brincker et al. (2001) and implementing it in MATLAB. The measurements from the five SYSCOM MS2003+ velocity transducers located along the length of the diaphragm (see Franquet 2010) were first filtered using a low pass Butterworth filter with a cut-off of 0.2 Hz to eliminate the low frequency drift. The Cross-Power Density function was then obtained at every discrete frequency and the singular value decomposition was computed. The first and second singular values were plotted over the range of frequencies to obtain the fundamental period using the standard peak-picking technique since the singular value at the fundamental period dominated. To reduce leakage resulting from the Fourier transform calculations during the FDD computation it was necessary to segment the signals to intervals of 2000 points and use a hamming window with an overlap of 50%. An output signal of 5 minutes or more was used for post-processing in order to obtain representative data from the structure. Modal Assurance Criterion (MAC) plots were used to validate the results of the determined modes and mode shapes. Fundamental periods were then converted into a diaphragm shear stiffness G' (kN/mm) for comparison with diaphragm design methodologies using the equation proposed by Medhekar and Kennedy (1999).

The results from the single-frequency excitation were used to obtain the values for the resonance plots (Figure 4). Each resonance plot was obtained from sine signals with eight different amplitudes at a single frequency (four shown). The relative velocity at the middle of the specimen was calculated using the average of the actuator velocity measurements to account for the possibility that the two actuators were not in phase. The velocity time-history was then plotted and the maximum amplitude of the steady-state response for each magnitude of excitation was determined. It was important to choose a representative portion of the steady-state response output as there was always a significant transient response after every change in excitation amplitude. The maximum values were then plotted on a single graph to provide curves that illustrate the range of resonant frequencies of the diaphragm (Figure 4).

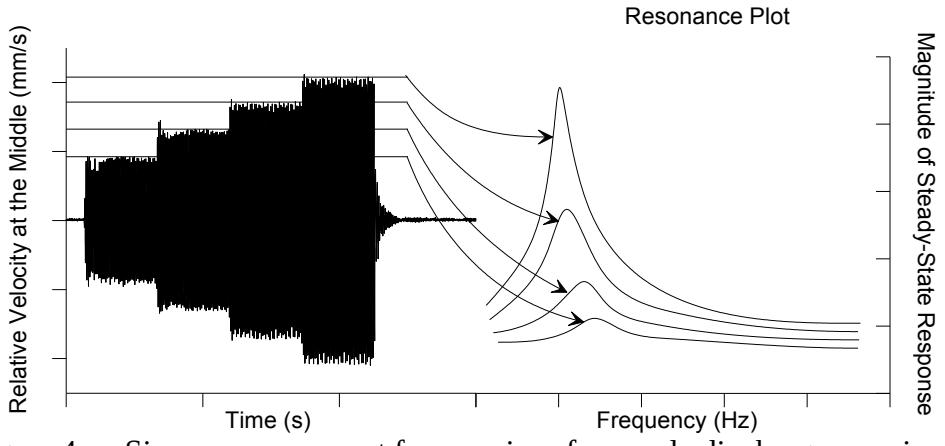

Figure 4. Sine sweep resonant frequencies of example diaphragm specimen.

Information regarding the shear force profile along the width of the diaphragm, as well as the deformation profile, was extracted from the seismic signals. The inertia forces along the width were first obtained by multiplying the acceleration measurements at every joist, and at the end beam parallel to the loading, by the respective tributary mass. See Franquet (2010) for the weights used for the purpose of this calculation.

The acceleration was derived from the displacements and filtered with a highpass Butterworth filter with a cut-off of 25 Hz to eliminate high frequency noise. The summation of these inertia forces over the width of the diaphragm, starting at midspan, yielded the shear force carried by the diaphragm at any particular joist location. Edge beam and actuator load cell and swivel weights were omitted from the inertia load calculation.

Results

The plots obtained from the white noise results (Figure 5) allowed for the quantification of the change in stiffness with increasing excitation amplitude. The results were normalized using the predicted diaphragm shear stiffnesses and strengths obtained with the SDI method for a single panel length (Luttrell 2004). Results show that the measured stiffness was greater than the predicted value at low amplitudes but decreased below the SDI shear stiffness at high amplitude excitations (Fig. 5b). The only exception in the testing program was for specimen DIA3 which was constructed with different end and interior connector patterns; in this case the SDI method greatly overestimated the shear stiffness (see Franquet 2010). The stiffness increase due to gypsum was also dependent on the amplitude of excitation. At the maximum white noise amplitude, the calculated difference was 28%. However, under high seismic excitations, the gypsum was shown to degrade and only the bare steel diaphragm stiffness remained.

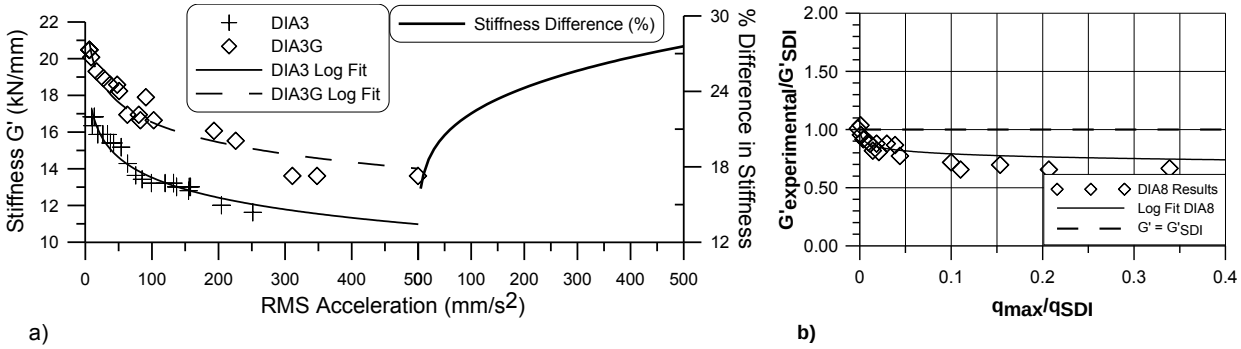

Figure 5. Example of white noise results: (a) change in stiffness vs. excitation amplitude; (b) $G'_{experimental}/G'_{SDI}$ vs. q_{max}/q_{SDI} for DIA8.

The shear force profiles of interest, which correspond to the force distributions that yield a maximum shear flow at a particular joist line, were plotted for examination. The concurrent deformed shapes were also plotted to observe the displacement demand imposed along the width of the diaphragm when the specimens were subjected to ground motion records. All specimens exhibited a high deformation demand over the first span at the location of maximum shear flow as illustrated in Figure 6.

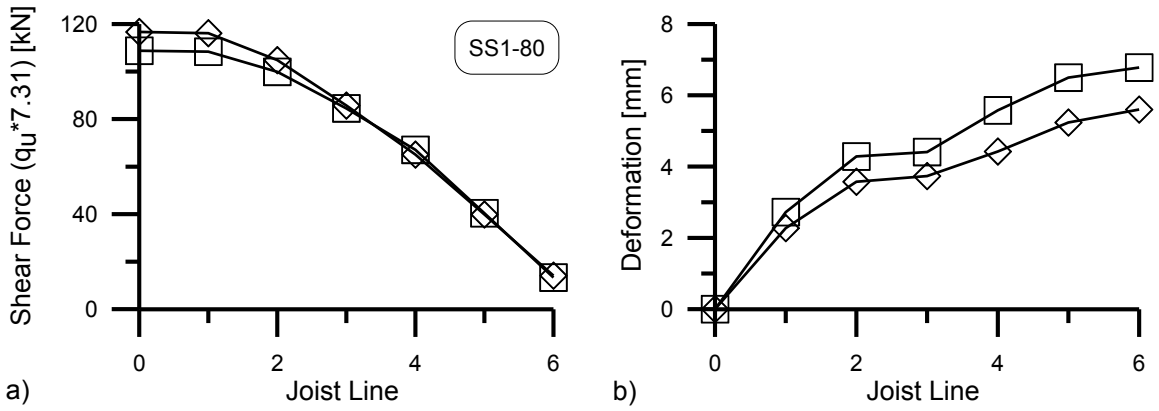

Figure 6. Typical shear force profile (a) and concurrent deformed shape (b).

The inelastic loading protocol resulted in pinched shear force vs. deformation hysteretic behaviour of the specimens due to bearing of the sheet steel around the nails and screws. Ultimate failure was characterized by the loss of a sidelap or frame fastener row due to excessive slotting around nails or pullout of a screwed sidelap span. In the case of the welded and button-punch specimen, detachment of the sidelap connections and fracture of the welds resulted in the overall loss of shear capacity of the specimen. A comparison of the failure patterns obtained with different frame fastener patterns and 0.76 mm decking is displayed in Figure 7. Figure 7a was used to contrast the failure pattern obtained with a 36/4 frame fastener pattern and 305 mm sidelap spacing. This earlier test was reported on by Tremblay et al. (2008a). The comparison shows that sidelap failure was not affected by a change in pattern. However, a decrease in nail failure along with a localization of the failure towards the ends was observed with increasing frame fastener pattern.

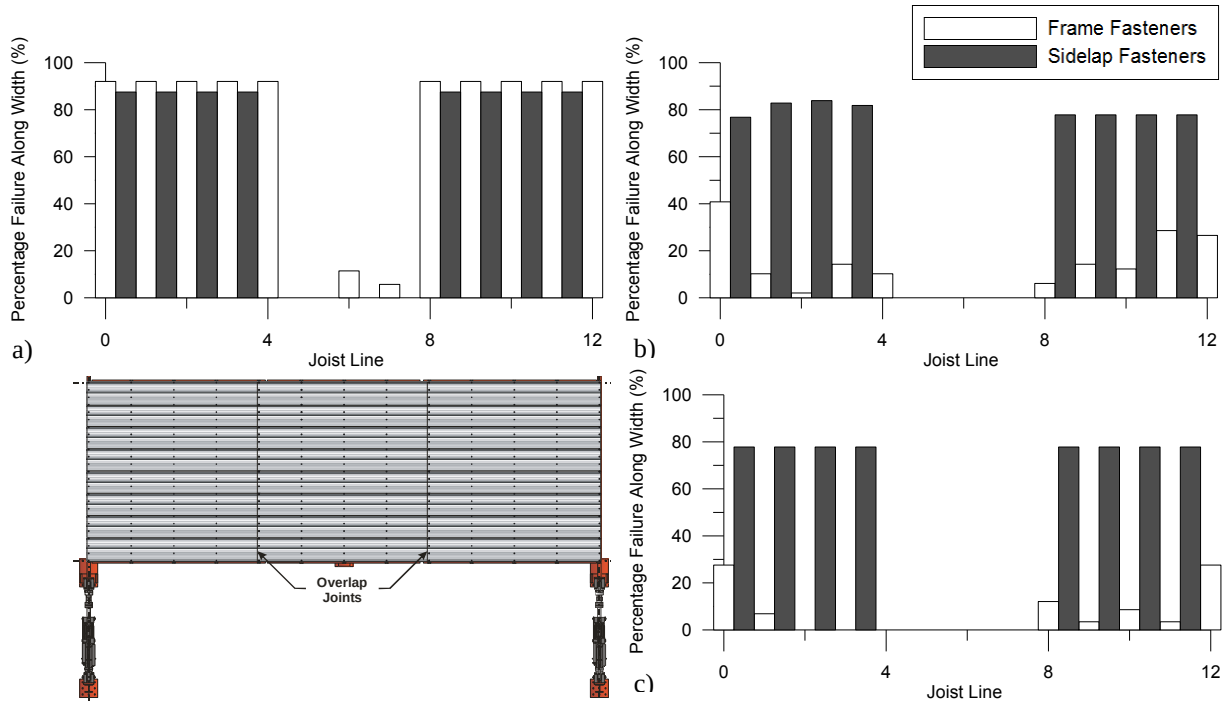

Figure 7. Failure pattern comparison for different frame fastener patterns with 0.76 mm deck thickness: DIA1 (a) (Tremblay et al. 2008a), DIA4 (b) and DIA5 (c)

The repair schemes allowed for the recuperation of the original shear resistance of the diaphragm specimens, however, variations in shear stiffness were noticed depending on the initial damage. Figure 8a displays typical hystereses for DIA7 and its repaired scenario with nail frame and rivet sidelap fasteners. Both diaphragms were able to maintain a maximum shear resistance for several cycles before experiencing any loss in capacity. In comparison, the welded and button-punch specimen, DIA10 (Figure 8b), reached a maximum shear resistance but soon afterwards experienced a degradation in both shear strength and stiffness. Such behaviour suggests that this specific fastener configuration would only exhibit a satisfactory dynamic response in its elastic range. A complete discussion of the performance of each diaphragm test specimen can be found in the report by Franquet (2010).

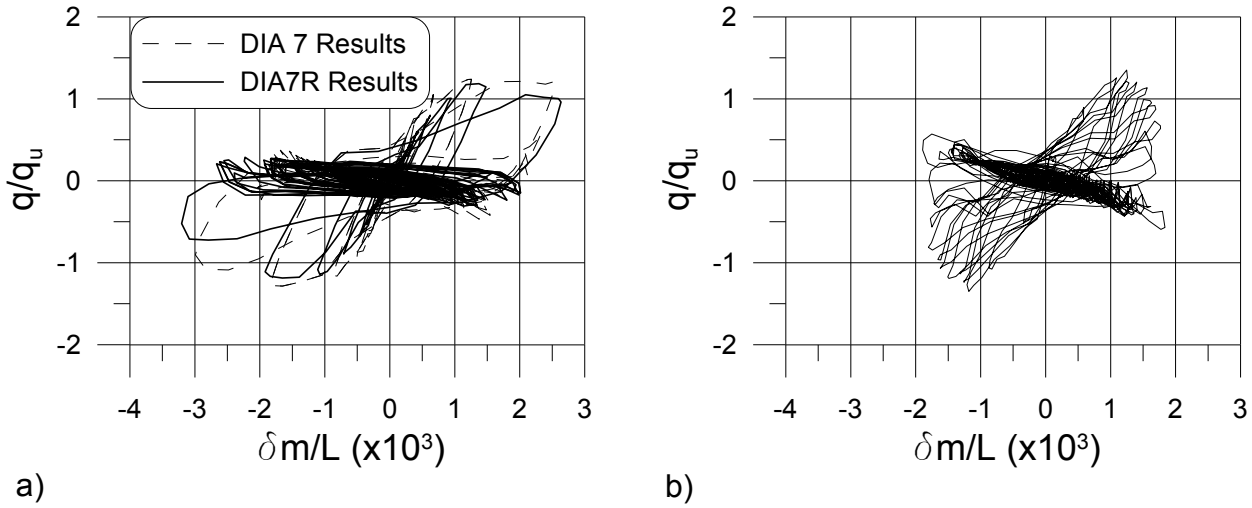

Figure 8. Hysteresis for DIA7 and DIA7R (a) and DIA10 (b); normalized shear load vs. displacement at centre divided by the length.

Conclusions

An experimental testing program on steel roof deck diaphragm assemblies was successfully carried out. Dynamic and seismic tests were conducted on eight diaphragm test specimens composed of corrugated deck sheeting with nail and screw or weld and button-punch frame and sidelap fasteners, respectively. The SDI method was determined to overestimate the shear stiffness at high amplitude excitations for all the specimens except for the case of different end and interior frame connector patterns. A maximum stiffness increase of 28% was recorded due to the addition of gypsum. The nailed and screwed specimens were shown to exhibit ductile pinched hysteretic behaviour while the welded and button-punched did not display much energy dissipation. The repair scenarios were successful at recuperating the original strength of the specimen. Further research should be completed to obtain the dynamic characteristics of diaphragms with other types of fasteners, thicker decks and different orientations.

Acknowledgements

Funding for this research was provided by the Natural Sciences and Engineering Research Council of Canada, the Vancouver Steel Deck Diaphragm Design Committee (VSDDC) and its many member companies (see Franquet 2010), the Canadian Sheet Steel Building Institute, the

Steel Deck Institute and Hilti Canada. Material for the test frame and specimens were provided by Hilti Canada Inc., Sofab Structural Steel Inc., Lainco and the Canam Group. The authors also wish to express their appreciation for the most valuable technical input from the industrial partners.

References

Brincker, R., Zhang, L., Andersen, P. (2001). Modal identification of output-only systems using frequency domain decomposition. *Smart Materials and Structures*, 10(3), 441-445.

Franquet, J.-E. (2010). Seismic design repair and retrofit strategies for steel roof deck diaphragms, MEng Thesis. Dept. of Civil Engineering & Applied Mechanics, McGill University, Montreal, QC.

Lamarche, C.-P., Proulx, J., Paultre, P., Turek, M., Ventura, C. E., Le, T. P., (2009). Toward a better understanding of the dynamic characteristics of single-storey braced steel frame buildings in Canada. *Canadian Journal of Civil Engineering,* 36(6), 969-979.

Luttrell, L. D. (2004). Diaphragm design manual (3rd ed.). Steel Deck Institute, Fox River Grove, Ill.

Mastrogiuseppe, S., Rogers, C.A., Nedisan, C.D., Tremblay, R. (2008). Influence of non-structural components on roof diaphragm stiffness and fundamental periods of single-storey steel buildings. *Journal of Constructional Steel Research*, 64(2), 214-227.

Medhekar, M. S., & Kennedy, D. J. L. (1999). Seismic evaluation of single-storey steel buildings. *Canadian Journal of Civil Engineering*, 26(4), 379-394.

NRCC (2005). National building code of Canada. National Research Council of Canada, Ottawa, ON.

Rogers, C.A., Tremblay, R., (2010), Impact of diaphragm behavior on the seismic design of low-rise steel buildings", AISC Engineering Journal. (In press)

Shrestha, K., Franquet, J., Rogers, C.A., Tremblay, R. (2009). OpenSees modeling of the inelastic seismic response of steel roof deck diaphragms, STESSA 2009 – 6th International Conference on the Behaviour of Steel Structures in Seismic Areas, Philadelphia, USA, 775-780.

Tremblay, R., Rogers, C.A. (2005). Impact of capacity design provisions and period limitations on the seismic design of low-rise steel buildings, *Int. J. of Steel Structures* 5(1), 1-22.

Tremblay, R., Rogers, C.A., and Nedisan, C. (2002). Use of uniform hazard spectrum and computed period in the seismic design of single-storey steel structures. *Proc. 7th US Nat. Conf. on Earthquake Eng.*, Boston, MA. Paper No. 195.

Tremblay, R., Martin, E., Yang, W., & Rogers, C. A. (2004). Analysis, testing and design of steel roof deck diaphragms for ductile earthquake resistance. *Journal of Earthquake Engineering*, 8(5), 775 - 816.

Tremblay, R., Rogers, C.A., Lamarche, C.-P., Nedisan, C.D., Franquet, J., Massarelli, R., Shrestha, K. (2008a). Dynamic seismic testing of large size steel deck diaphragms for low-rise building applications, 14th World Conference on Earthquake Engineering, Beijing, China. Paper No. 05-05-0066.

Tremblay, R., Nedisan, C.D., Lamarche C.-P., Rogers, C.A. (2008b). Periods of vibration of a low-rise building with a flexible steel roof deck diaphragm. *Proc. 5th Int. Conf. on Thin-Walled Structures*, Brisbane, Australia, 615-622.